Magneto-orientation and quantum size effects in spin-polarized STM conductance in the presence of a subsurface magnetic cluster

Ye. S. Avotina,[1] Yu. A. Kolesnichenko,[1] and J. M. van Ruitenbeek[2]
[1]*B.I. Verkin Institute for Low Temperature Physics and Engineering, National Academy of Sciences of Ukraine, 47 Lenin Avenue, 61103 Kharkov, Ukraine*
[2]*Kamerlingh Onnes Laboratorium, Universiteit Leiden, Postbus 9504, 2300 Leiden, The Netherlands*
(Received 7 July 2009; revised manuscript received 25 August 2009; published 29 September 2009)

The influence of a single magnetic cluster in a nonmagnetic host metal on the spin current $\mathbf{j}^{(s)}$ and the charge current $\mathbf{j}$ in the vicinity of a ferromagnetic scanning tunneling microscope (STM) tip is studied theoretically. Spin-flip processes due to electron interaction with the cluster are taken into account. We show that quantum interference between the partial waves injected from the STM tip and those scattered by the cluster results in the appearance of components perpendicular to the initial polarization of the spin current $\mathbf{j}^{(s)}$, which obtain a strongly inhomogeneous spatial distribution. This interference produces oscillations of the conductance as a function of the distance between the contact and the cluster center. The oscillation amplitude depends on the current polarization. We predict a strong magneto-orientational effect; the conductance oscillations may grow, shrink, or even vanish for rotation of the cluster magnetic moment $\boldsymbol{\mu}_{\mathrm{eff}}$ by an external magnetic field. These results can be used for the determination of the $\boldsymbol{\mu}_{\mathrm{eff}}$ for magnetic clusters below a metal surface.

DOI: 10.1103/PhysRevB.80.115333 PACS number(s): 61.72.J−, 73.40.Cg, 73.63.Rt, 74.50.+r

I. INTRODUCTION

Subsurface defects, such as impurities and vacancies, result in oscillations of the conductance as a function of the position of a scanning tunneling microscope (STM) tip relative to the defect position (see, for example, Refs. 1–3). These Friedel-type oscillations originate from interference between electron waves directly transmitted through the contact and waves that are scattered by the defect and reflected back by the contact. The theory of STM conductance in the presence of a single nonmagnetic pointlike defect below a metal surface in the vicinity of the contact has been developed in Refs. 4 and 5. First the signature of Fermi-surface anisotropy in STM conductance in the presence of defects had been analyzed theoretically in detail in Ref. 6. In the paper[7] the general results of Ref. 6 was applied for the theoretical investigation of the conductance of a tunnel point contact of noble metals in the presence of a single defect below surface. A pattern of the conductance oscillations, which can be observed by the method of scanning tunneling microscopy, was obtained for different orientations of the surface for the noble metals.[7] Recently it had been confirmed experimentally that Fermi surfaces can be imaged in real space with a low-temperature scanning tunneling microscope when subsurface point scatterers are present.[8] The effect of Kondo scattering by a subsurface magnetic impurity on the conductance of a tunnel point contact has been analyzed theoretically in Ref. 9.

The applicability of STM can be extended for the study of magnetic objects below the surface of a conductor when a magnetic material is used for the STM tip such that the electric current is spin polarized (SP) (for review of SP-STM see Ref. 10). An important feature of SP-STM is that the spin-polarized current influences a magnetic object in a nonmagnetic matrix, producing so-called spin-transfer torque (for review, see Ref. 11). For example, near a point contact, where the current density is large, the spin-transfer torque can be strong enough to reorient the magnetization of ferromagnetic layers in magnetic multilayers.[12] Such investigations are very important for the development of innovative high-density data-storage technologies.

In this paper we consider theoretically the conductance of a tunnel point contact between magnetic and nonmagnetic metals in a SP-STM geometry. A magnetic cluster is embedded in the nonmagnetic metal in the vicinity of the contact. The changes in the spin-polarized current and the spin-transfer torque that influences the magnetic moment of the cluster are analyzed. We study the dependence of the amplitude of the conductance oscillations as a function of the STM tip position on the relative orientation between the spin polarization of the tunneling electrons and the magnetic moment of the cluster $\boldsymbol{\mu}_{\mathrm{eff}}$.

II. MODEL OF THE CONTACT AND BASIC EQUATIONS

Let us consider a tunnel contact between a semi-infinite half space $z \geq 0$ of a nonmagnetic metal (the sample) and a sharp tip of a magnetic conductor (Fig. 1). A voltage V is applied between the tip and the sample. The electrical (and spin) current flows through a small region of the surface at $z=0$ near the tip apex that is closest to the sample. This system models the geometry of a SP-STM experiment. The tip magnetization (in real SP-STM the magnetization of the last atom[10]), which we choose along the z direction, defines the direction of the polarization of the tunnel current. Such magnetization can be obtained, for example, for a Fe/Gd-coated W STM tip.[13] In the nonmagnetic metal we place a spherical single-domain magnetic cluster having a magnetic moment μ_{eff} (Fig. 1). As first predicted by Frenkel and Dorfman[14] particles of a ferromagnetic material are expected to organize in a single magnetic domain below a critical particle size (a typical value for this critical size for Co is about 35 nm). Depending on the size and the material, the magnetic moments of such particles can be μ_{eff}

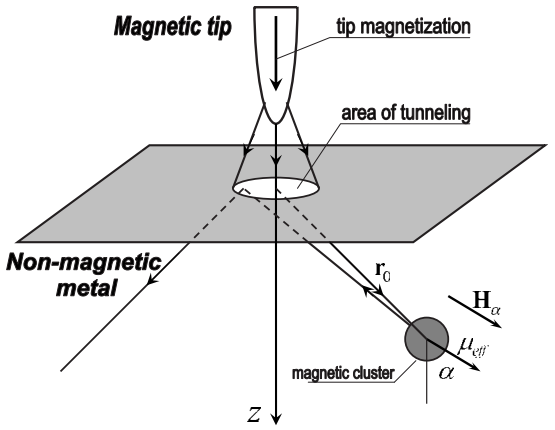

FIG. 1. Model of the contact in a SP-STM configuration with a subsurface magnetic cluster near the tunnel contact point. Spin-polarized electrons tunnel into the nonmagnetic metal in the small area below the STM tip. The trajectories of electrons that are scattered by the spherical magnetic cluster are shown schematically.

$\sim 10^2-10^5$ μ_B, where μ_B is the Bohr magneton.[15] Below, we only consider electron scattering by the magnetic cluster, assuming the mean-free paths for all other processes (electron-spin-diffusion length, electron-phonon mean-free path and others) are much larger than the distance between the contact and the cluster center r_0.

In order to describe the spin-polarized electron states of our system we use the approach proposed in the works of Slonczewski and Berger:[16,21] all calculations are performed by means of independent single-particle spinor wave functions $\hat{\Psi}(\mathbf{r}_l;\sigma_l)$ of electrons with opposite spin directions, where $\mathbf{r}_l$ and σ_l are the position vector and the spin direction, respectively, for each spin orientation $l=1,2$. We use the representation $\sigma_{1,2}=\uparrow,\downarrow$ in which the spin projection on the z axis, $s_z=\pm\frac{1}{2}$, is used. This approach corresponds to reducing the many-particle problem of a partially polarized electron system with nonzero average spin to a double-particle problem for electrons in a pure (completely polarized) spin state. Neglect of electron-electron interactions enables us to separate the double-particle Schrödinger equation into two independent equations for $\hat{\Psi}(\mathbf{r}_l;\sigma_l)$. In our case this separation is valid if $\mu_{\text{eff}} \gg \mu_B$, i.e., the electron-electron exchange interaction is negligible compared to electron exchange interaction with the cluster. Generally, the moment $\boldsymbol{\mu}_{\text{eff}}$ of the cluster in a nonmagnetic metal takes an arbitrary direction. This direction (the angle α in Fig. 1) can be held fixed by an external magnetic field $\mathbf{H}_\alpha$, the value of which is estimated as $H_\alpha \simeq T/\mu_{\text{eff}}$, where T is the temperature (see, for example, Ref. 17). For $\mu_{\text{eff}} \simeq 10^2 \mu_B$ and $T \sim 1$ K the field H_α is on the order of 0.1 T. We assume that H_α is much smaller than the magnetocrystalline anisotropy field of the STM tip, i.e., the direction of the external magnetic field controls the direction of the cluster magnetic moment but its influence on the spin-polarization of the STM current is negligible. If the magnetic moment $\boldsymbol{\mu}_{\text{eff}}$ of the cluster is "frozen" by the field H_α the problem becomes a stationary one. Also we take the distance between the contact and the cluster r_0 to be much smaller than the radius $r_H = cp_F/eH_\alpha$ of the electron trajectory in the applied external magnetic field H_α, and we do not take into account trajectory magnetic effects, which have been analyzed in Ref. 18. The condition $r_0 \ll r_H$ together with inequality $\mu_B H_\alpha/\varepsilon \ll 1$ (ε is the electron energy) allow neglecting the magnetic field in the single-electron Hamiltonian and considering $\mathbf{H}_\alpha$ as an independent external parameter.

The external magnetic field may result in a modulation of the tunnel current due to electron-spin precession.[19] For our problem such precession would become noticeable when the transit time for the electron motion from the contact to the cluster $t \simeq r_0/v_F$ is larger than $1/\omega_L$, where v_F and ω_L are the Fermi velocity and Larmor frequency. The inequality mentioned above, $r_0 \ll r_H$, is equivalent to the condition $\omega_L t \ll 1$, so that the effect of electron-spin precession is negligible.

Thus, under the assumptions outlined above the spinor wave functions $\hat{\Psi}(\mathbf{r}_l;\sigma_l)$ satisfy the one-electron Schrödinger equation

$$\left(-\frac{\hbar^2}{2m^*}\nabla_l^2 - \varepsilon\right)\hat{I}\hat{\Psi}(\mathbf{r}_l;\sigma_l) = -\hat{U}(\mathbf{r}_l)\hat{\Psi}(\mathbf{r}_l;\sigma_l), \tag{1}$$

where m^* is the effective mass of the electrons and $\hat{U}(\mathbf{r})$ is the interaction potential of the electrons with the cluster. The matrix $\hat{U}$ consists of two parts, describing the potential as well as the magnetic scattering,

$$\hat{U}(\mathbf{r}) = \left(g\hat{I} + \frac{1}{2\mu_B} J\boldsymbol{\mu}_{\text{eff}}\hat{\boldsymbol{\sigma}}\right) D(|\mathbf{r}-\mathbf{r}_0|), \tag{2}$$

where g is the constant describing the nonmagnetic part of the interaction (for $g>0$ the potential is repulsive), J is the constant of exchange interaction, $\boldsymbol{\mu}_{\text{eff}} = \mu_{\text{eff}}(\sin\alpha, 0, \cos\alpha)$ is the magnetic moment of the cluster, $\hat{\boldsymbol{\sigma}} = (\hat{\sigma}_x, \hat{\sigma}_y, \hat{\sigma}_z)$ with $\hat{\sigma}_\mu$ the Pauli matrices and $\hat{I}$ is the unit matrix. $D(|\mathbf{r}-\mathbf{r}_0|)$ is a spherically symmetric function localized within a region of characteristic radius r_D centered at the point $\mathbf{r}=\mathbf{r}_0$, which satisfies the normalization condition

$$\int d\mathbf{r}' D(\mathbf{r}') = 1. \tag{3}$$

Equation (1) must be supplemented with the common boundary conditions for continuity of the wave function and its normal derivative on the metal surface.

We assume that the potential $\hat{U}(\mathbf{r})$ is small and use perturbation theory. As a first step we should find the solutions $\hat{\Psi}^{(0)}(\mathbf{r}_l;\sigma_l)$ of Eq. (1) for $\hat{U}(\mathbf{r})=0$. Generally, this solution depends on the model chosen to represent the tunnel barrier. For any suitable model for the potential barrier the wave functions $\hat{\Psi}^{(0)}(\mathbf{r}_l;\sigma_l)$ describe the spreading of the electron waves in the metal from the small contact region on the surface. Here, we use the results of Refs. 9 and 20, in which the tunnel contact is modeled in the form of a circular orifice of radius a, with a large amplitude potential barrier $U_0\delta(z)$.

In order to describe the spin polarization of the STM current we introduce different magnitudes for the wave vector $\mathbf{k}_\sigma$ for spin-up and spin-down electrons (for the same energy ε) before tunneling from the tip. This difference results in

different amplitudes $t(\mathbf{k}_\sigma)$ of the electron waves injected into the nonmagnetic metal for different directions of the spin,[9,20]

$$t_\sigma(\mathbf{k}_\sigma) \approx \frac{\hbar^2 k_\sigma \cos\vartheta}{im^* U_0}; \quad |t_\sigma| \ll 1. \tag{4}$$

Here, ϑ is the angle between wave vector $\mathbf{k}_\sigma$ and the normal to the surface $z=0$, pointing into the sample. The total effective polarization P_{eff} of the current depends on the difference between the probabilities of tunneling for different σ,

$$P_{\text{eff}}(\varepsilon) = \frac{|t_\uparrow|^2 - |t_\downarrow|^2}{|t_\uparrow|^2 + |t_\downarrow|^2} = \frac{k_\uparrow^2 - k_\downarrow^2}{k_\uparrow^2 + k_\downarrow^2}. \tag{5}$$

The functions $\hat{\Psi}^{(0)}(\mathbf{r}_l;\sigma_l)$ for each spin direction have the same spatial dependence as those for a contact between nonmagnetic metals. In following calculations we use the asymptotic expression for $\hat{\Psi}^{(0)}(\mathbf{r}_l;\sigma_l)$ valid for $ka \ll 1$ (Ref. 9)

$$\hat{\Psi}^{(0)}(\mathbf{r};\sigma) = t_\sigma \Psi^{(0)}(\mathbf{r})\hat{\psi}_\sigma, \tag{6}$$

where

$$\Psi^{(0)}(\mathbf{r}) = \frac{(ka)^2 z}{2ikr^2} e^{ikr}\left(1 + \frac{1}{ikr}\right), \tag{7}$$

$\hat{\psi}_\sigma$ is the spinor

$$\hat{\psi}_\uparrow = \begin{pmatrix} 1 \\ 0 \end{pmatrix}, \quad \hat{\psi}_\downarrow = \begin{pmatrix} 0 \\ 1 \end{pmatrix}, \tag{8}$$

and $k=\sqrt{2m^*\varepsilon}/\hbar$ is the magnitude of the electron wave vector $\mathbf{k}$ in the nonmagnetic metal. Note that the wave function $\Psi^{(0)}(\mathbf{r})$, Eq. (7), is zero in all points on the surface $z=0$, except the point $r=0$ (at the contact) where it diverges. This divergence is the result of taking the limit $a \to 0$ in the integral expressions for $\Psi^{(0)}(\mathbf{r})$.[5,20] Yet, Eq. (7) gives a finite value for the total charge current through the contact as obtained over a half sphere of radius r with its center in the point $\mathbf{r}=0$ for $r \to 0$.

The solution to Eq. (1) in linear approximation in the potential $\hat{U}$, Eq. (2), can be written as

$$\hat{\Psi}(\mathbf{r};\sigma) = t_\sigma\{\Psi^{(0)}(\mathbf{r})\hat{\psi}_\sigma + [(\tilde{g} \pm \tilde{J}\cos\alpha)\hat{\psi}_\sigma + \tilde{J}\sin\alpha\hat{\psi}_{-\sigma}]\Psi^{(1)}(\mathbf{r})\}, \tag{9}$$

where the sign $(\pm)$ corresponds to $\sigma=\uparrow,\downarrow$. We have introduced the notation

$$\tilde{g} = \frac{2m^* k}{\hbar^2} g, \quad \tilde{J} = \frac{m^* k}{\mu_B \hbar^2} J\mu_{\text{eff}} \tag{10}$$

for the dimensionless constants of interaction for potential and magnetic scattering, respectively. The wave function scattered by the cluster is given by

$$\Psi^{(1)}(\mathbf{r}) = -\frac{1}{k}\int d\mathbf{r}' G_0^+(\mathbf{r},\mathbf{r}') D(|\mathbf{r}' - \mathbf{r}_0|)\Psi^{(0)}(\mathbf{r}'), \tag{11}$$

which undergoes specular reflection at the metal surface. Aiming for a solution for the wave function $\hat{\Psi}_{\boldsymbol{\sigma}}(\mathbf{r})$ in first approximation in the small parameter $|t_\sigma| \ll 1$ we substitute the electron Green's function $G_0^+(\mathbf{r},\mathbf{r}')$ of the nonmagnetic half space in Eq. (9),

$$G_0^+(\mathbf{r},\mathbf{r}') = G_{00}^+(|\mathbf{r} - \mathbf{r}'|) - G_{00}^+(|\mathbf{r} - \tilde{\mathbf{r}}'|), \tag{12}$$

where $\tilde{\mathbf{r}}=(\boldsymbol{\rho},-z)$ is the mirror image of the point $\mathbf{r}$ relative to the metal surface and G_{00}^+ is the Green's function for free electrons,

$$G_{00}^+(R) = -\frac{e^{ikR}}{4\pi R}; \quad R = |\mathbf{r} - \mathbf{r}'|. \tag{13}$$

The wave function, Eq. (9), enables calculation of the charge-current density $\mathbf{j}$ and spin-current density $\mathbf{j}^{(\mu)}$, and the expectation value of the spin $\mathbf{s}$. They are obtained as the sums of independent contributions of the two electron groups $(l=1,2)$

$$\mathbf{j}(\mathbf{r}) = \frac{e\hbar}{m^*}\sum_{l=1,2} \text{Im}(\hat{\Psi}\nabla\hat{\Psi}^+)_{\mathbf{r}_1=\mathbf{r}_2=\mathbf{r}}, \tag{14}$$

$$\mathbf{j}^{(\mu)}(\mathbf{r}) = \frac{i\hbar}{2m^*}\sum_{l=1,2} [(\nabla\hat{\Psi}^+)\sigma_\mu\hat{\Psi} - \hat{\Psi}^+\sigma_\mu(\nabla\hat{\Psi})]_{\mathbf{r}_1=\mathbf{r}_2=\mathbf{r}}, \tag{15}$$

$$\mathbf{s}(\mathbf{r}) = \sum_{l=1,2} (\hat{\Psi}^+\hat{\boldsymbol{\sigma}}\hat{\Psi})_{\mathbf{r}_1=\mathbf{r}_2=\mathbf{r}}. \tag{16}$$

The Eqs. (14)–(16) with wave function, Eq. (9), describe the so-called tunneling contributions (see, Ref. 16). They are proportional to the tunneling probability and define the measurable quantities which can be obtained after averaging over the energies of the tunneling electrons and wave-vector directions (see, Sec. III).

In absence of the cluster $s_x=s_y=0$ and the local magnetization $\mathbf{s}_0(\mathbf{r})$ due to itinerant spin-polarized electrons is oriented along the z axis. The spin polarization in zeroth approximation, $s_{z0}(\mathbf{r})$, which is calculated from the wave function, Eq. (6), is a monotonic function of coordinates

$$s_{z0}(\mathbf{r}) = (|t_\uparrow|^2 - |t_\downarrow|^2)\left(\frac{kza^2}{2r^2}\right)^2\left[1 + \frac{1}{(kr)^2}\right]. \tag{17}$$

The electron scattering by the spin-dependent potential, Eq. (2), changes the value and the direction of the vector $\mathbf{s}_0(\mathbf{r})$. Components s_x and s_y appear due to electron scattering by the cluster and they are subject to quantum interference between transmitted and scattered waves. As a result of the interference the spin components perpendicular to the z axis are oscillatory functions of the coordinates while s_{z0} acquires a small oscillatory component proportional to $\tilde{J}^2$.

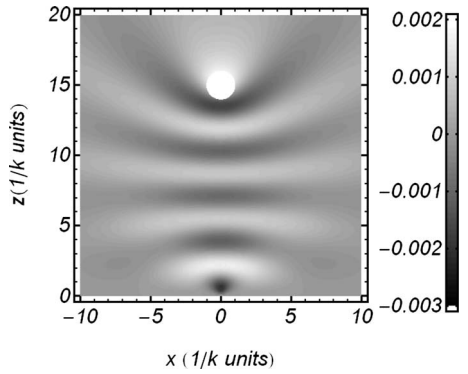

FIG. 2. Grayscale plot of the spacial distribution of the x component of the spin density, $s_x(\mathbf{r})/c_0$. The coordinate plane xz in real space crosses the contact and the cluster of the radius $r_D=k^{-1}$ with its center in the point $\mathbf{r}_0=(0,0,15)k^{-1}$.

$$\begin{bmatrix} s_x(\mathbf{r}) \\ s_y(\mathbf{r}) \end{bmatrix} = (|t_\uparrow|^2 \pm |t_\downarrow|^2)\tilde{J} \sin\alpha |\Psi^{(0)}(\mathbf{r})||\Psi^{(1)}(\mathbf{r})| \times \begin{Bmatrix} \cos \\ \sin \end{Bmatrix} [\varphi_1(\mathbf{r}) - \varphi_0(\mathbf{r})]. \quad (18)$$

Here $|\Psi^{(i)}(\mathbf{r})|$ and $\varphi_i(\mathbf{r})$ are the absolute values and the phases of the coordinate part of the wave functions, Eq. (9) [see, Eqs. (7) and (11)].

Figure 2 shows the spacial distribution of the x component of the normalized spin density $s_x(\mathbf{r})/c_0$ in the vicinity of the contact. The normalization constant $c_0=(|t_\uparrow|^2+|t_\downarrow|^2)\tilde{J}(ka)^4 \sin\alpha/16\pi$. The figure demonstrates that the spin component $s_x(\mathbf{r})$ changes sign in the space of the normal metal. The sign of s_x depends on the difference of the phases $\varphi_i(\mathbf{r})$. In Fig. 3 we present a vector plot of the x component of the spin-current density $\mathbf{j}^{(x)}$. An intricate image of the distribution in orientation of $\mathbf{j}^{(x)}$ is visible. Note the lines at which the direction of the vector $\mathbf{j}^{(x)}$ is inverted.

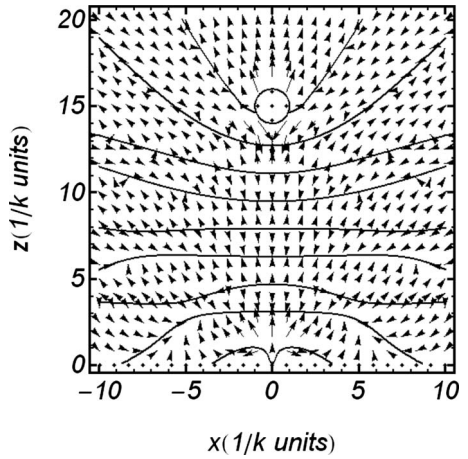

FIG. 3. Vector plot of the direction of the x component of spin-current density, $\mathbf{j}^{(x)}$. The contour lines correspond to $j_z^{(x)}=0$. The plane xz crosses the contact and the cluster; as in Fig. 2 we have chosen $r_D=k^{-1}$ and $\mathbf{r}_0=(0,0,15)k^{-1}$.

III. CONDUCTANCE OF THE CONTACT, SPIN CURRENT, AND SPIN-TRANSFER TORQUE

The total current through the contact can be evaluated by integration of the charge current density $\mathbf{j}(\mathbf{r})$, Eq. (14), over a half sphere centered at the point contact $r=0$ and covering the contact at $z>0$, and integration over all directions of the electron wave vector on the Fermi surface $\varepsilon=\varepsilon_F$. In the Ohm's law approximation and at zero temperature the total current through the contact I can be written as

$$I = eV\rho(\varepsilon_F)r^2 \int_{\varepsilon=\varepsilon_F} \frac{d\Omega_\mathbf{k}}{4\pi} \int d\Omega \Theta(z)\Theta(k_z) j_r(\mathbf{r}), \quad (19)$$

where $d\Omega$ and $d\Omega_\mathbf{k}$ are elements of solid angle in real and momentum space, respectively, $\rho(\varepsilon_F)$ is the electron density of states at the Fermi energy, ε_F, for one spin direction, k_z is z component of the wave vector, $j_r(\mathbf{r})$ is the radial component of $\mathbf{j}(\mathbf{r})$, Eq. (14), and $\Theta(x)$ is the Heaviside unit step function. After integration of Eq. (19) the conductance G of the contact takes the form

$$G = \frac{I}{V} = G_0 \left[1 + \frac{6}{\pi}(\tilde{g} + P_{\text{eff}}\tilde{J}\cos\alpha) W(\mathbf{r}_0) \right]_{\varepsilon=\varepsilon_F}, \quad (20)$$

where G_0 is the conductance of the contact in absence of the cluster

$$G_0 = (k_{F\uparrow}^2 + k_{F\downarrow}^2)\frac{e^2\hbar^3(k_F a)^4}{72\pi(m^* U_0)^2}. \quad (21)$$

Here, $k_{F\sigma}$ and k_F are the absolute values of electron wave vectors at the Fermi level in magnetic and nonmagnetic metals, respectively; P_{eff} is the effective spin polarization of the current injected through the contact [see Eq. (5)]; the constants $\tilde{g}$ and $\tilde{J}$ are given by Eq. (10) and

$$W(\mathbf{r}_0) = \int d\mathbf{r}' D(|\mathbf{r}' - \mathbf{r}_0|)\left(\frac{z'}{r'}\right)^2 y_1(kr') j_1(kr'), \quad (22)$$

where $j_l(x)$ and $y_l(x)$ are the spherical Bessel functions. Equation (20) coincides with the result for a tunnel point contact between nonmagnetic metals[9] when $P_{\text{eff}}=0$ and $kr_D \ll 1$. When the radius of action r_D of the function $D(|\mathbf{r}-\mathbf{r}_0|)$ is much smaller than the distance between the contact and the cluster center r_0, $W(\mathbf{r}_0)$ is an oscillatory function of kr_0 for $kr_D \geq 1$, but the oscillation amplitude is reduced as a result of superposition of waves scattered by different points of the cluster. The integral $W(\mathbf{r}_0)$, Eq. (22), can be calculated asymptotically for $r_0 \gg r_D$, $kr_0 \gg 1$, and $kr_D \gtrsim 1$. For a homogeneous spherical potential $D(|\mathbf{r}|)=V_D^{-1}\Theta(r_D-r)$ (V_D is the cluster volume) the function $W(\mathbf{r}_0)$ takes the form

$$W(\mathbf{r}_0) \simeq \frac{3}{2}\left(\frac{z_0}{r_0}\right)^2 \frac{\sin 2kr_0}{(2kr_0)^2} \frac{j_1(kd)}{kd}, \quad (23)$$

where $d=2r_D$ is the cluster diameter. The last factor in Eq. (23) describes the quantum size effect related with electron reflections by the cluster's boundary. Such oscillations may exist if the cluster boundary is sharp on the scale of the electron wavelength. Figure 4 shows the dependence of the amplitude of the conductance oscillations on the cluster di-

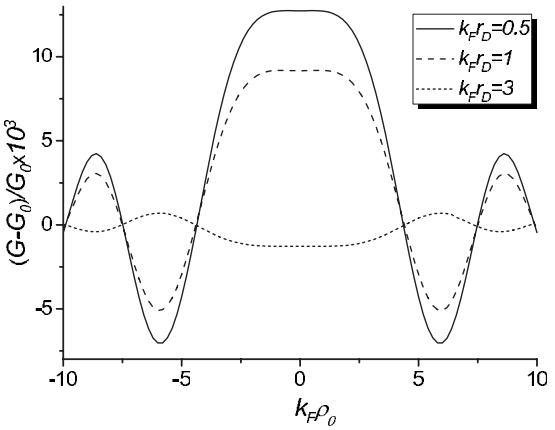

FIG. 4. Dependence of the oscillatory part of the conductance on the tip position on the metal surface for different cluster diameters. The ρ_0 coordinate is measured from the point $\rho_0=0$ at which the contact is situated directly above the cluster; $r_0=(0,0,10)/k_F$; $\tilde{g}=0.5$; $\tilde{J}=2.5$; $P_{\text{eff}}=0.4$; and $\alpha=0$.

ameter. It demonstrates that a π-phase shift may occur resulting from interference of electron waves over a distance of the cluster diameter.

In Eq. (20) the term proportional to P_{eff} takes into account the difference in the probabilities of scattering of electrons with different σ by the localized magnetic moment μ_{eff}. It depends on the angle α between the tip magnetization and $\boldsymbol{\mu}_{\text{eff}}$ as cos α. The same dependence was first predicted for a tunnel junction between ferromagnets for which the magnetization vectors are misaligned by an angle α,[16] and this was observed in SP-STM experiments.[10]

Similar to the electrical conductance, Eq. (20), the total spin current for each spin component can be calculated

$$I^{(z)} = \frac{G_0 V}{e}\left[P_{\text{eff}} + \frac{6}{\pi}(P_{\text{eff}}\tilde{g} + \tilde{J}\cos\alpha)W(\mathbf{r}_0)\right]_{\varepsilon=\varepsilon_F}, \quad (24)$$

$$I^{(x)} = \frac{6G_0 V}{e\pi}\sin\alpha[\tilde{J}W(\mathbf{r}_0)]_{\varepsilon=\varepsilon_F}. \quad (25)$$

For our choice of the vector $\boldsymbol{\mu}_{\text{eff}}$, $I^{(y)}=0$. The value of the z component of the spin current $I^{(z)}$, Eq. (24), is determined to a large extent by the polarization P_{eff}, Eq. (5), of the initial current. The oscillatory part of $I^{(z)}$ is modified by the addition of a term due to spin-flip processes on the cluster. The spin-current component perpendicular to initial direction of polarization, $I^{(x)}$, has only a term that oscillates with r_0 and which disappears when the magnetic moment $\boldsymbol{\mu}_{\text{eff}}$ is aligned with the z direction.

The spin-transfer torque $\mathbf{T}$ acting on the magnetic moment $\boldsymbol{\mu}_{\text{eff}}$ is given by

$$\mathbf{T} = -\frac{J}{\hbar}\int d\mathbf{r}' D(|\mathbf{r}' - \mathbf{r}_0|)\boldsymbol{\mu}_{\text{eff}} \times \langle \mathbf{s}(\mathbf{r}')\rangle, \quad (26)$$

where

$$\langle \mathbf{s}(\mathbf{r})\rangle = eV\rho(\varepsilon_F)\int_{\varepsilon=\varepsilon_F}\frac{d\Omega_{\mathbf{k}}}{4\pi}\mathbf{s}(\mathbf{r}), \quad (27)$$

$\mathbf{s}(\mathbf{r})$ is defined by Eq. (16). This torque is related with the spin-polarized electron tunnel current. In linear approximation in $\tilde{J}$ only the spin-density contribution $s_{z0}(\mathbf{r})$, Eq. (17), without interaction with the cluster, should be taken for the calculation of the torque, Eq. (26). In this approach $T_x=T_z=0$. For large $r_0 \gg r_D$ we obtain

$$T_y = \sin\alpha\frac{3G_0 V}{e\pi}\left\{P_{\text{eff}}\tilde{J}\left(\frac{z_0}{kr_0^2}\right)^2\left[1+\frac{1}{(kr_0)^2}\right]\right\}_{\varepsilon=\varepsilon_F}. \quad (28)$$

The dependence of T_y, Eq. (28), on the angle α agrees with the dependence of the spin-transfer torque in tunnel junctions between two ferromagnets with different directions of magnetization.[16,21]

In this paper we do not aim to investigate the dynamics of the cluster magnetic moment. We only note that once the spin-polarized current-induced torque pulls the magnetic moment away from alignment with H_α, the cluster moment will start precessing around the field axis. The Larmor frequency is defined by the magnetic field due to combining the external field H_α and the effective field produced by the polarized current $H_{\text{eff}} \simeq -J\langle \mathbf{s}(\mathbf{r}_0)\rangle / g_c\mu_B$ (g_c is the cluster "g factor"). The precession of the cluster magnetic moment gives rise to a time modulation of the SP-STM current as for clusters on a sample surface.[22,23] The study of nonstationary effects provides a further means of obtaining information on the cluster and the spin polarization of the current inside the sample.

IV. DISCUSSION

In summary, we have studied theoretically the current and spin flows through a tunnel point contact between magnetic and nonmagnetic metals when the tunnel current is spin polarized in the geometry of SP-STM, Fig. 1. Electron-spin-flip processes due to a magnetic cluster situated in the nonmagnetic metal have been taken into account. These processes result in the appearance of components of the spin-current density $\mathbf{j}^{(s)}(\mathbf{r})$ perpendicular to the source direction (taken along the contact axis z), and a finite expectation value of the spin $\mathbf{s}(\mathbf{r})$. We have analyzed the contribution of tunneling electrons to the spacial distribution of $\mathbf{j}^{(x,y)}(\mathbf{r})$ and $s_{x,y}(\mathbf{r})$. It is found that these are nonmonotonic functions of the coordinates and undergo strong spacial oscillations originating from quantum interference between partial waves transmitted through the contact and those scattered by the cluster (see, Figs. 2 and 3). Specifically, between the contact and the cluster there are neighboring regions in which $\mathbf{j}^{(x)}(\mathbf{r})$ flows in opposite directions (Fig. 3).

The oscillatory correction, ΔG, to the conductance G_0 of the ballistic tunnel point contact strongly depends on the magnetic scattering, Eq. (20),

$$\Delta G \sim (\tilde{g} + P_{\text{eff}}\tilde{J}\cos\alpha)\sin 2kr_0, \quad kr_0 \gg 1. \quad (29)$$

The effective spin polarization P_{eff} of the tunneling electrons and the dimensionless constants of potential scattering $\tilde{g}$ and

exchange scattering $\tilde{J}$ are given by Eqs. (5) and (10). Generally, for a single magnetic defect, which has a magnetic moment on the order of one Bohr magneton, μ_B, the spin part of electron scattering gives only a small contribution to the electrical resistance. For a magnetic cluster with $\mu_{\text{eff}} \gg \mu_B$, the exchange energy can be larger than the energy of spin-independent interaction [$\tilde{J} > \tilde{g}$, see Eq. (10)]. An interesting phenomenon may be found when $P_{\text{eff}}\tilde{J} \geq \tilde{g}$. A change in the direction of the vector $\boldsymbol{\mu}_{\text{eff}}$ (the angle α) controlled by an external magnetic field is predicted to lead to a change in the amplitude of the oscillations, and for certain directions the amplitude may vanish, $G_{osc}=0$. This large magneto-orientational effect provides a new mechanism for obtaining information on magnetic particles buried below a metal surface. Note that this effect is observable only for a spin-polarized current: if $t_\uparrow = t_\downarrow$, in linear approximation in $\tilde{J}$ the changes in the scattering amplitude for spin-up and spin-down electrons balance each other and the magneto-orientational effect is absent.

As a consequence of spin flips due to the interaction of the electrons with the cluster the oscillatory part $\Delta I^{(z)}$ of the spin current in the original z direction obtains a correction which depends on the exchange constant $\tilde{J}$ and the orientation of the magnetic moment, Eq. (24)

$$\Delta I^{(z)} \sim (P_{\text{eff}}\tilde{g} + \tilde{J}\cos\alpha)\sin 2k_F r_0, \quad k_F r_0 \gg 1. \tag{30}$$

A component of the spin current perpendicular to the z direction, $I_x^{(s)}$, is formed only by scattered waves and as the result of quantum interference it becomes an oscillatory function of the distance r_0, Eq. (25)

$$I^{(x)} \sim \tilde{J}\sin\alpha \sin 2k_F r_0, \quad k_F r_0 \gg 1. \tag{31}$$

The spin currents, Eqs. (30) and (31), appear even in the case of nonpolarized current through the contact and they are related to the magnetic scattering by the cluster.

The torque, which acts on the magnetic cluster due to spin polarization of electric current is a monotonic function of the distance r_0, Eq. (28), to linear approximation in the exchange constant

$$T_y \sim \sin\alpha P_{\text{eff}}\tilde{J}(z_0/k_F r_0^2)^2, \quad k_F r_0 \gg 1, \tag{32}$$

where z_0 is the depth of the cluster below metal surface.

These results may be exploited in future experiments for detecting and investigating individual magnetic clusters buried below the surface of a host metal. Specifically, a comparison of the amplitude of the conductance oscillations for different directions of the cluster magnetic moment allows determination of the exchange energy $J\mu_{\text{eff}}$ and for a known value of the exchange integral J to find μ_{eff}.

ACKNOWLEDGMENTS

One of us (Yu.K) would like to acknowledge useful discussions with B. I. Belevtsev, A. B. Beznosov, N. F. Kharchenko, and D. I. Stepanenko. This research was supported partly by the program "Nanosystems nanomaterials and nanotechnology" of National Academy of Sciences of Ukraine and Fundamental Research State Fund of Ukraine (Project No. F 25.2/122).

[1] N Quaas, M Wenderoth, A Weismann, R. G. Ulbrich and K Schönhammer, Phys. Rev. B **69** 201103(R) (2004).
[2] M. Schmid, W. Hebenstreit, P. Varga, and S. Crampin, Phys. Rev. Lett. **76**, 2298 (1996).
[3] O. Kurnosikov, O. A. O. Adam, H. J. M. Swagten, W. J. M. de Jonge, and B. Koopmans, Phys. Rev. B **77**, 125429 (2008).
[4] K. Kobayashi, Phys. Rev. B **54**, 17029 (1996).
[5] Ye. S. Avotina, Yu. A. Kolesnichenko, A. N. Omelyanchouk, A. F. Otte, and J. M. van Ruitenbeek, Phys. Rev. B **71**, 115430 (2005).
[6] Ye. S. Avotina, Yu. A. Kolesnichenko, A. F. Otte, and J. M. van Ruitenbeek, Phys. Rev. B **74**, 085411 (2006).
[7] Ye. S. Avotina, Yu. A. Kolesnichenko, S. B. Roobol, and J. M. van Ruitenbeek, Low Temp. Phys. **34**, 207 (2008).
[8] A. Weismann, M. Wenderoth, S. Lounis, P. Zahn, N. Quaas, R. G. Ulbrich, P. H. Dederichs, and S. Blügel, Science **323**, 1190 (2009).
[9] Ye. S. Avotina, Yu. A. Kolesnichenko, and J. M. van Ruitenbeek, J. Phys.: Condens. Matter **20**, 115208 (2008).
[10] M. Bode, Rep. Prog. Phys. **66**, 523 (2003).
[11] J. Z. Sun and D. C. Ralph, J. Magn. Magn. Mater. **320**, 1227 (2008).
[12] M. Tsoi, A. G. M. Jansen, J. Bass, W. C. Chiang, M. Seck, V. Tsoi, and P. Wyder, Phys. Rev. Lett. **80**, 4281 (1998).
[13] A. Kubetzka, M. Bode, O. Pietzsch, and R. Wiesendanger, Phys. Rev. Lett. **88**, 057201 (2002).
[14] J. Frenkel and J. Dorfman, Nature (London) **126**, 274 (1930).
[15] S. Chikazumi, *Physics of Ferromagnetism* (Oxford University Press, New York, 1999).
[16] J. C. Slonczewski, Phys. Rev. B **39**, 6995 (1989).
[17] S. V. Vonsovsky, *Magnetism* (John Wiley & Sons, New York, 1974).
[18] Ye. S. Avotina, Yu. A. Kolesnichenko, A. F. Otte, and J. M. van Ruitenbeek, Phys. Rev. B **75**, 125411 (2007).
[19] F. J. Jedema, H. B. Heersche, A. T. Fllip, L. L. A. Baselmans, and B. J. van Weels, Nature (London) **416**, 713 (2002).
[20] I. O. Kulik, Yu. N. Mitsai, and A. N. Omelyanchouk, Zh. Eksp. Teor. Fiz. **63**, 1051 (1974).
[21] L. Berger, Phys. Rev. B **54**, 9353 (1996).
[22] H. C. Manoharan, Nature (London) **416**, 24 (2002).
[23] C. Durkan and M. E. Welland, Appl. Phys. Lett. **80**, 458 (2002).